A Model for Jellyfish Detritus Decay through Microbial Processing

Filip Strniša, Gregor Kosec
"Jožef Stefan" Institute, Parallel and Distributed Systems Laboratory, Ljubljana, Slovenia
filip.strnisa@ijs.si, gregor.kosec@ijs.si

***Abstract*—The decay of jellyfish blooms introduces a significant organic matter source to the local marine environment that has still an unknown impact on the ecosystem. In recent laboratory experiments, authors studied how the introduction of excess organic material affects the coastal pelagic microbiome by introducing *Aurelia aurita* detritus to jars of seawater. During these experiments they have monitored bacterial abundance, amino acids' concentrations, dissolved organic carbon, as well the build-up of some inorganic nutrients. They have found, that about half of the protein-rich organic matter in jellyfish detritus is almost instantly available to microbes as dissolved organic matter. Based on this experimental data we devised a mathematical model of the jellyfish proteins (amino acids) degradation caused by marine bacteria. The model is built on top of the Monod bacterial growth model and the Luedeking-Piret metabolite production model. In addition, we incorporated the bacterial populations' age to model the lag phase as well as bacterial decay. In this paper, we demonstrate that with the proposed model, we can sufficiently describe the laboratory measurements.**

***Keywords*—bacterial growth; Monod model; Luedeking-Piret model; jellyfish**

I. Introduction

Jellyfish blooms can significantly influence the nutrient cycles in the ocean, and their eventual decay may result in a large release of both organic and inorganic nutrients [1]. As jellyfish organic matter is rich in protein [2] and consequently in nitrogen, it may be of particular interest to investigate how bacterial mineralization affects the local nitrogen cycle. Fixed nitrogen is often considered one of the limiting nutrients in marine environments [3], [4].

The Monod model is often the growth model of choice when modelling microbial ecology [5]. The said model is generally used to describe how a microorganism's specific growth rate is related to substrate concentration. In batch systems, where the amount of substrate present is limited, the bacterial growth can be described in several phases: the lag phase, the exponential growth phase, the steady-state phase, and finally, the decay phase (Fig. 1). The lag phase occurs while the microorganism adapts to the environment after inoculation and may be caused by the change of temperature, culture age, and other factors. Once the microorganism successfully adapts to the environment, it begins to multiply exponentially. The exponential growth may come to its end because of one or several of the following factors: product inhibition, oxygen or substrate depletion. Following the exponential growth phase is the steady-state phase, where no net biomass growth can be observed due to equal amount of decaying and newly grown microorganisms. Finally, net biomass growth becomes negative as the biomass starts decaying faster than it grows due to lack of available nutrients, which marks the onset of the decay phase.

The authors would like to acknowledge the financial support of Slovenian Research Agency (ARRS) in the framework of the research core funding No. P2-0095 and project J7-2599.

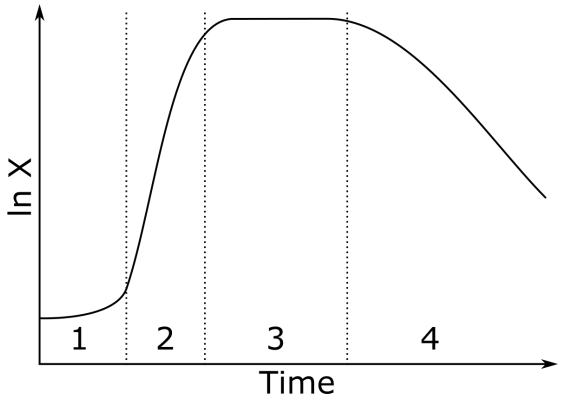

Figure 1. A sketch of bacterial growth phases. $\ln X$ is the natural logarithm of bacterial biomass. The phases are as follows: 1 — lag phase; 2 — exponential growth phase; 3 — steady-state phase; 4 — decay phase.

Typically used bacterial growth models incorporate the exponential growth, and sometimes also bacterial decay [5]. However, such models are unable to predict the lag phase, although several approaches exist for modelling this phenomenon [6]. These approaches however do not incorporate cell age, for which it has been suggested that it may affect the metabolic efficiency of the cell [7]. In literature a model has been developed, which builds on this idea, but it did not incorporate it specifically for the purpose of modelling the lag phase [8].

In this paper, we develop a simple bacterial growth model that considers biomass, as well as substrate, and product concentrations. Following the results of experiments, where a specific jellyfish species *Aurelia aurita* was considered [2], we assume the amino acids being released from jellyfish detritus to be the limiting nutrient in marine bacteria growth, which through the process of mineralization produce ammonium. The model incorporates the Monod growth kinetics with substrate consumption, bacterial ageing and decay, as well as Luedeking-

Piret model for product formation. Cell age is included in the model to enable us to model the lag phase. The model is then fitted to one set of the experimental data and validated with another set.

II. Experiments

Microbial degradation of dead jellyfish organic matter was studied in a laboratory simulated scenario [2]. The jellyfish species used in the experiments was *Aurelia aurita* . Two experiments were performed where key parameters, i.e. bacterial abundance, dissolved organic carbon (DOC), dissolved nitrogen (DN), and amino acid concentrations, as well as inorganic nutrients' concentrations were monitored. Among the inorganic nutrients monitored in the experiments were: ammonium, nitrate, nitrite, and phosphate. Each experiment was performed in 3 parallels, each in a separate jar of 5-10 L in volume. Additionally, there were control experiments performed at the same time, also in 3 parallels. The growth medium used was filtered seawater, which contained a representative pool of marine bacteria, and the experiments were inoculated by the addition of a specified amount of jellyfish organic matter. The amount of jellyfish organic matter added at the inoculation was such that it reflected a typical decay of *Aurelia aurita* [2]. Analyses of the jellyfish organic matter suggest, that about half of it is in form of dissolved organic matter, and the rest is particulate organic matter. The former is almost exclusively available for the marine bacteria on site. A significant portion of this dissolved organic matter is in form of combined and free amino acids.

First (E1) of the two experiments was focused on capturing the whole process, including the initial exponential growth, as well as the later bacterial decay phase, while the second (E2) focused only on the exponential growth phase. The time frames of the two experiments were 0-84 h, and 0-32 h, respectively. The experiments are described in greater detail in [2].

The results of the experiments are graphed in Fig. 2, where normalized concentrations of bacterial abundance, amino acids, ammonium (one of the inorganic nutrients), and DOC are plotted against time. All concentrations are subtracted by the control experiments' mean value of these concentrations to better highlight the changes. In Fig. 2a we can see that bacterial abundance follows a typical bacterial growth curve (Fig. 1). Additionally we can observe that amino acids, and DOC are being consumed during the experiments, whereas ammonium is produced. It is important to note however, that amino acids contribute to DOC as they contain carbon. Once the amino acids are depleted in E1, the DOC concentration also stops dropping significantly, which suggests that the amino acids may have been the primary or limiting substrate involved in the growth process. A noticeable lag phase can be observed in E2's bacterial abundance plot (Fig. 2b). The experiments' results additionally indicate that *Pseudoalteromonas*, *Alteromonas*, and *Vibrio* species are the dominating active bacteria during the detritus degradation, making up the majority of bacterial abundance during the exponential growth phase and the decay phase [2]. Although big part of jellyfish organic matter is processed by marine bacteria within 1.5 days, the metabolites released by these bacteria may further cause nutrient imbalances in the local ecosystem.

Fig. 2 excludes the DN data, as they combine dissolved organic nitrogen as well as dissolved inorganic nitrogen. Amino acids contribute to the former, while ammonium contributes to the latter, which makes it difficult to draw trends from the DN data. Also excluded from the plots are nitrate, and nitrite concentrations (both inorganic dissolved nitrogen) Their concentrations remain mostly unchanged throughout the experiments [2].

The experiments described above involved bacterial growth, as well as biochemical change of a material. They were performed in well mixed 5-10 L vessels, where oxygen levels were kept above the critical concentration, at which aerobic bacteria slow down their reproduction. We can regard such as setup as a homogeneous batch bioreactor in which an aerobic bioprocess is taking place. In our batch bioreactor model the jellyfish detritus acts as the substrate (S), while the bacteria stand for the active biomass (X), and ammonium is a chemical product of the bioprocess (P). Although other chemical species contribute to DOC as well, amino acids appear to be the limiting substrate. Therefore amino acids act as S in our model. As mentioned above, the bacteria involved in jellyfish organic matter degradation are *Pseudoalteromonas*, *Alteromonas*, and *Vibrio*, but for simplicity, these are all regarded as a part of one variable X.

III. Model

The simplest set of balances to describe the process is one following only X (bacterial abundance) and S (amino acids):

$$\frac{dX}{dt} = \mu\left(S\right) X, \tag{1}$$

$$\frac{dS}{dt} = -\frac{\mu\left(S\right) X}{Y_{X/S}}, \tag{2}$$

where we use the Monod growth model:

$$\mu = \mu_{max} \frac{S}{K_S + S}. \tag{3}$$

μ is the specific growth rate of X, and μ_{max} is the maximal specific growth rate of X, $Y_{X/S}$ is the biomass yield from substrate S (how much new X appears for the amount of S consumed), and finally K_S is the Monod substrate saturation constant, which is actually and inverse measure of the microorganism's (X) affinity towards S. A sketch of Eq. (3) is displayed in Fig. 3, indicating that at low S ($S \ll K_S \rightarrow \mu = \frac{\mu_{max}}{K_S} S$) the growth is of first order in regards to S, and at high S ($S \gg K_S \rightarrow \mu = \mu_{max}$) it is of zeroth order in regards to S. The model represented by Eqs. (1)-(3) is however incapable of reproducing the whole growth curve as there is no decay term in X's balance, and since all the involved

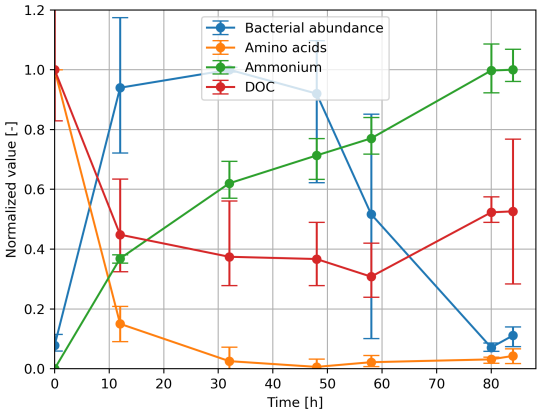

(a) Experiment 1 results.

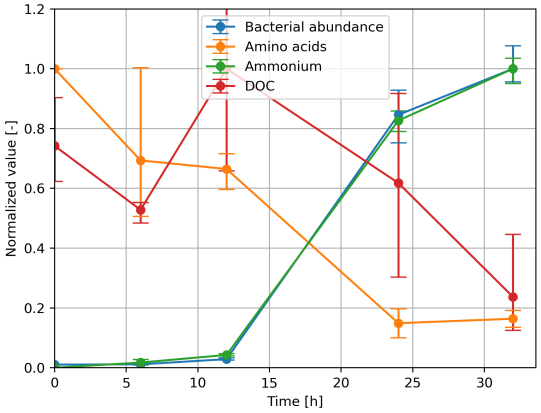

(b) Experiment 2 results.

Figure 2. Experimental results plotted against time. Bacterial abundance — normalized bacterial abundance, Amino acids — normalized amino acid concentration, Ammonium — normalized ammonium ion concentration; DOC — normalized DOC concentration; a: experiment 1; b: experiment 2. The normalized values were computed as $\bar{c_t} = \frac{c_t - c_C}{max(c) - c_C}$, where c is a placeholder variable representing the datasets (Bacterial abundance, Amino acids, Ammonium, DOC), c_t is c at a discrete point in time t, c_C is the average value from the control experiments (baseline), and $max(c)$ is the maximum value of the dataset. The maximum values of datasets were 1.16×10^7 cells mL^{-1}, $10\,\mu\mathrm{mol\,L}^{-1}$, and $12.2\,\mu\mathrm{mol\,L}^{-1}$ for bacterial abundance, amino acid concentration, and ammonium ion concentration, rescpectively [2].

variables and parameters can only be positive, X can only increase or stagnate. Therefore a decay term needs to be introduced to Eq. (1). Additionally, in experiment 2 there is a significant lag phase noticeable in the growth curve (see Fig. 2), which the model above cannot reproduce if it is using parameters obtained from a fit on experiment 1. Literature suggests that differently aged microorganism have different μ_{max}, and K_S as their metabolic efficiency may decrease with cell age [7], [8]. It is through this idea that the lag phase could be modelled. We have chosen to break down X into 3 age-groups: young, mature, and old (represented by indices 0, 1, and 2, respectively). The current model assumes handicaps for μ_{max} only, and K_S is unchanged for all age-groups. The decay parameter is also varied between the age-groups. We can also add the

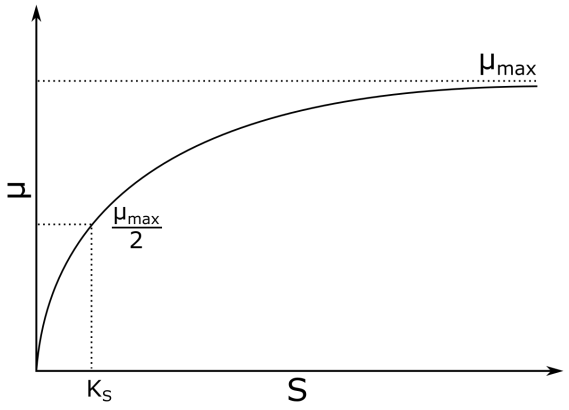

Figure 3. A sketch of the specific growth rate μ against substrate concentration S, following the Monod growth model (Eq. (3)). μ is asymptotically approaching the maximal specific growth rate μ_{max}, as S increases. At low S we thus observe first order growth, and at high S zeroth order growth. Also displayed is the Monod substrate saturation constant, K_S. It can be found at $\mu = \frac{\mu_{max}}{2}$.

product (P, ammonium) formation to the model. This follows the Luedeking-Piret model [9]. Accounting for these assumptions we write the following balances:

$$\frac{\mathrm{d}X_0}{\mathrm{d}t} = \sum_{i=0}^{2} \mu_i X_i - a^\star X_0 - d_0 X_0, \tag{4}$$

$$\frac{\mathrm{d}X_1}{\mathrm{d}t} = a^\star X_0 - a^\star X_1 - d_1 X_1, \tag{5}$$

$$\frac{\mathrm{d}X_2}{\mathrm{d}t} = a^\star X_1 - d_2 X_2, \tag{6}$$

$$\frac{\mathrm{d}S}{\mathrm{d}t} = -\frac{\sum_{i=0}^{2} \mu_i X_i}{Y_{X/S}}, \tag{7}$$

$$\frac{\mathrm{d}P}{\mathrm{d}t} = \alpha \sum_{i=0}^{2} \mu_i X_i + \beta \sum_{i=0}^{2} X_i. \tag{8}$$

$a^\star$ is the ageing parameter, d_i is the decay parameter of the i-th age-group, α is the growth associated coefficient of the Luedeking-Piret equation, and β is its non-growth associated counterpart. X's age-groups have separate balances, where growth (cell division) only directly impacts the population of young cells, whereas maturation is achieved by the ageing coefficient $a^\star$, and finally decay by d_i.

IV. Results

We solve the system of Ordinary Differential Equations (ODE) Eq. (4)-(8) with initial conditions displayed in Table I. Initial values of X, and S are taken from experimental results [2]. Parameters μ_{max}, $a^\star$, K_S, d, $Y_{X/S}$, α, β, and w are manipulated to fit the model to E1 results.

w is an arbitrary constant used to determine the age-distribution of the population of X (i.e. $w = 0 \rightarrow$ all are young, $w = 1 \rightarrow$ all are old, $w = 0.5 \rightarrow$ most

are mature, some are young and old). The fitted model is presented in Fig. 4a, with fitted parameters listed in Table II. This fit was obtained manually, by graphing the model alongside the experimental results with Python. A series of user-manipulatable sliders was programmed to be included with the plot, which could then be manually adjusted, while the graphs were updated in real time.

The same parameters were then used to model E2. One can notice, that E2's initial X is almost 8-times smaller than E1's, but according to the model, this did not cause the initial lag in E2, as the model and experiment did not agree. However, by changing w to a higher value (making the bacterial culture older), we get the fit presented in Fig. 4b. This adjustment can be justified by the fact, that E1 and E2 were performed a week apart, the latter being performed later, and with environmental samples drawn simultaneously, therefore we can assume that the E2 culture was indeed older.

The fits of S and P appear mostly accurate. However, modelling the decay, and the steady-state phases of X remains a challenge. w was successfully utilized to simulate the lag phase. In E2 the modelled S appears to fit less accurately to the experiments, but this may very well come down to experimental errors.

The fit results suggest that in these particular experiments the bacterial doubling time ($t_d = \frac{\ln 2}{\mu_{max}}$) is about 2.2 h, which seems to be in line with typical bacterial doubling times observed in nature [10]. Also according to the fit, on average a single bacterial cell uses up about 8×10^{-10} mol of amino acids to grow and divide. Assuming that a model bacterium weighs about 1×10^{-12} g, and its dry weight is about 40 % thereof [11], with further 50 % of this dry weight being protein [12], there should be on average about 2×10^{-13} g of protein per bacterial cell. We can estimate that on average an amino acid's molecular weight is about 110 Da, so converting 8×10^{-10} mol to grams, we get about 7×10^{-12} g of amino acids consumed by a cell before it divides. Comparing the theoretically assumed protein content of 2×10^{-13} g cell^{-1} with amino acid consumption of 7×10^{-12} g cell^{-1}, we can assume that the value of $Y_{X/S}$ is not unreasonable, albeit this result would suggest that most of the metabolized amino acids are not used to build new bacteria, but rather for energy production.

TABLE I. MODEL INITIAL CONDITIONS.

Variable	E1	E2
$X(t=0)$	$X_{init}(w^2-2w+1, -2w^2+2w, w^2)$	
X_{init}	8.7×10^5 cells mL^{-1}	1.2×10^5 cells mL^{-1}
$S(t=0)$	10 µmol L^{-1}	
$P(t=0)$	0 µmol L^{-1}	

TABLE II. FITTING RESULTS*.

Parameter	Value
μ_{max} [h^{-1}]	0.32 (0: μ_{max}; 1: 0.95μ_{max}; 2: 0.25μ_{max})
$a^\star$ [h^{-1}]	0.075
K_S [µmol L^{-1}]	2.8
d [h^{-1}]	0.058 (0: 0.01d; 1: 0.05d; 2: d)
$Y_{X/S}$ [cells L µmol^{-1} mL^{-1}]	1.24×10^6
α [µmol mL cell^{-1} L^{-1}]	6.54×10^{-7}
β [µmol mL cell^{-1} L^{-1} h^{-1}]	2.8×10^{-8}
w [-]	E1: 0; E2: 0.7

*Obtained by fitting the proposed model (Eqs. 4-8) onto E1 data. In brackets 0, 1, and 2 stand for young, mature, and old age-groups, respectively.

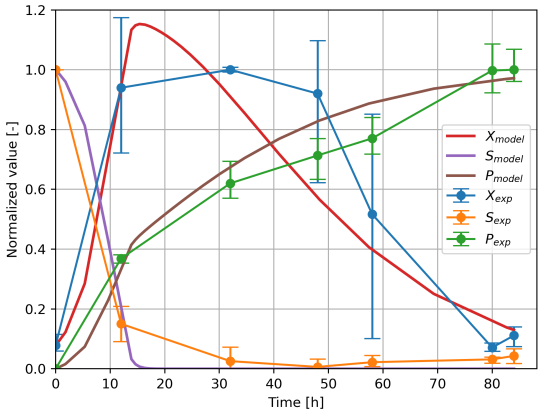

(a) Experiment 1 model fit results.

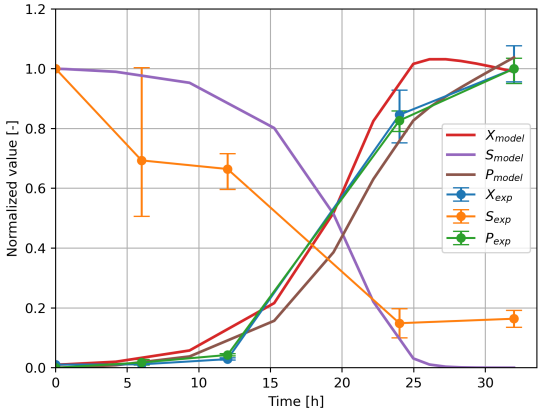

(b) Experiment 2 model fit results.

Figure 4. Fit results plotted with experimental results for comparison against time. X — normalized bacterial abundance, S — normalized amino acid concentration, P — normalized ammonium concentration. Indices $model$ and exp represent model and experiments' results, respectively. The normalized values are computed as in Fig. 2, model values are normalized to maximum experimental values. The parameters were first fitted to E1 results, and then the same parameters were used to model E2. E2 fit was improved by changing the w value. These parameters are presented in Table II.

V. CONCLUSION

We have presented a simple model for jellyfish detritus decay. The model is a work-in-progress, and is looking to be updated and improved as we move forward. Currently the model is based on treating all bacteria involved as a single biomass variable X, as substrate S we employed the cumulative concentration of all amino acids, and the lone product P considered here is ammonium. This

simplified model is currently able to accurately capture substrate uptake as well as product formation, and the exponential phase of biomass growth, including the lag phase. The model however struggles to reproduce the plateau of the stagnant biomass growth phase, and the biomass decay phase. Further additions to the model could include the consideration of separate bacterial species, several substrates, and continuous treatment of the cell age. The improved model will also include additional metabolites, which were omitted in this work, e.g. phosphate.

REFERENCES

[1] K. A. Pitt, D. T. Welsh, and R. H. Condon, "Influence of jellyfish blooms on carbon, nitrogen and phosphorus cycling and plankton production," *Hydrobiologia*, vol. 616, no. 1, pp. 133–149, Jan 2009.

[2] T. Tinta, Z. Zhao, A. Escobar, K. Klun, B. Bayer, C. Amano, L. Bamonti, and G. J. Herndl, "Microbial processing of jellyfish detritus in the ocean," *Frontiers in Microbiology*, vol. 11, p. 2638, 2020.

[3] C. M. Moore, M. M. Mills, K. R. Arrigo, I. Berman-Frank, L. Bopp, P. W. Boyd, E. D. Galbraith, R. J. Geider, C. Guieu, S. L. Jaccard, T. D. Jickells, J. La Roche, T. M. Lenton, N. M. Mahowald, E. Marañón, I. Marinov, J. K. Moore, T. Nakatsuka, A. Oschlies, M. A. Saito, T. F. Thingstad, A. Tsuda, and O. Ulloa, "Processes and patterns of oceanic nutrient limitation," *Nature Geoscience*, vol. 6, no. 9, pp. 701–710, Sep 2013.

[4] S. Pajares and R. Ramos, "Processes and microorganisms involved in the marine nitrogen cycle: Knowledge and gaps," *Frontiers in Marine Science*, vol. 6, p. 739, 2019.

[5] M. Wade, J. Harmand, B. Benyahia, T. Bouchez, S. Chaillou, B. Cloez, J.-J. Godon, B. Moussa Boudjemaa, A. Rapaport, T. Sari, R. Arditi, and C. Lobry, "Perspectives in mathematical modelling for microbial ecology," *Ecological Modelling*, vol. 321, pp. 64–74, 2016.

[6] I. Swinnen, K. Bernaerts, E. Dens, A. Geeraerd, and J. Van Impe, "Predictive modelling of the microbial lag phase: a review," *INTERNATIONAL JOURNAL OF FOOD MICROBIOLOGY*, vol. 94, no. 2, pp. 137–159, JUL 15 2004.

[7] E. J. Stewart, R. Madden, G. Paul, and F. Taddei, "Aging and death in an organism that reproduces by morphologically symmetric division," *PLOS Biology*, vol. 3, no. 2, 02 2005.

[8] V. Lavric and D. W. Graham, "Birth, growth and death as structuring operators in bacterial population dynamics," *Journal of Theoretical Biology*, vol. 264, no. 1, pp. 45 – 54, 2010.

[9] A. Garnier and B. Gaillet, "Analytical solution of Luedeking–Piret equation for a batch fermentation obeying Monod growth kinetics," *Biotechnology and Bioengineering*, vol. 112, no. 12, pp. 2468–2474, 2015.

[10] B. Gibson, D. J. Wilson, E. Feil, and A. Eyre-Walker, "The distribution of bacterial doubling times in the wild," *Proceedings of the Royal Society B: Biological Sciences*, vol. 285, no. 1880, p. 20180789, 2018.

[11] G. Bratbak and I. Dundas, "Bacterial dry matter content and biomass estimations." *Applied and Environmental Microbiology*, vol. 48, no. 4, pp. 755–757, 1984.

[12] M. Simon and F. Azam, "Protein-content and protein-synthesis rates of planktonic marine-bacteria," *Marine Ecology Progress Series*, vol. 51, no. 3, pp. 201–213, Feb 6 1989.